Stem Cell Reports, Volume *10*

Supplemental Information

Human Induced Pluripotent Stem Cell-Derived Cardiac Cell Sheets Expressing Genetically Encoded Voltage Indicator for Pharmacological and Arrhythmia Studies

Naim Shaheen, Assad Shiti, Irit Huber, Rami Shinnawi, Gil Arbel, Amira Gepstein, Noga Setter, Idit Goldfracht, Amit Gruber, Snizhanna V. Chorna, and Lior Gepstein

Supplemental Figures and Figure Legends

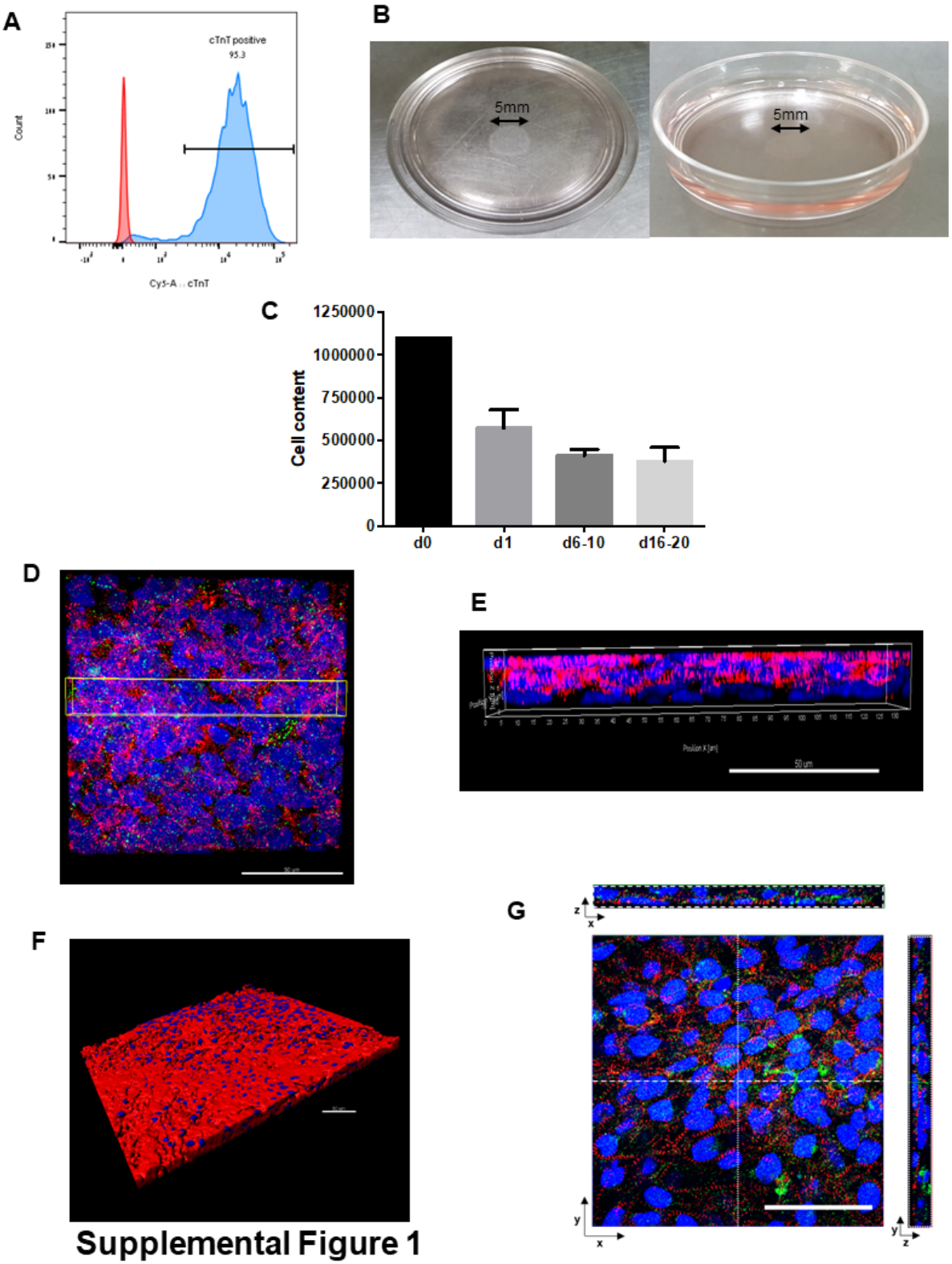

Supplemental Figure 1

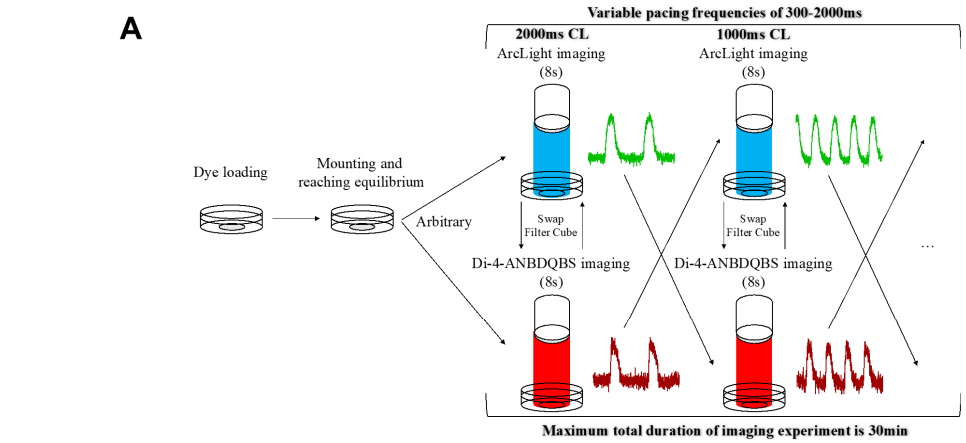

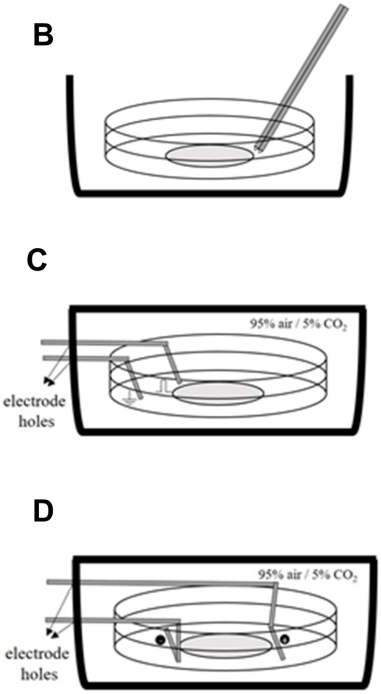

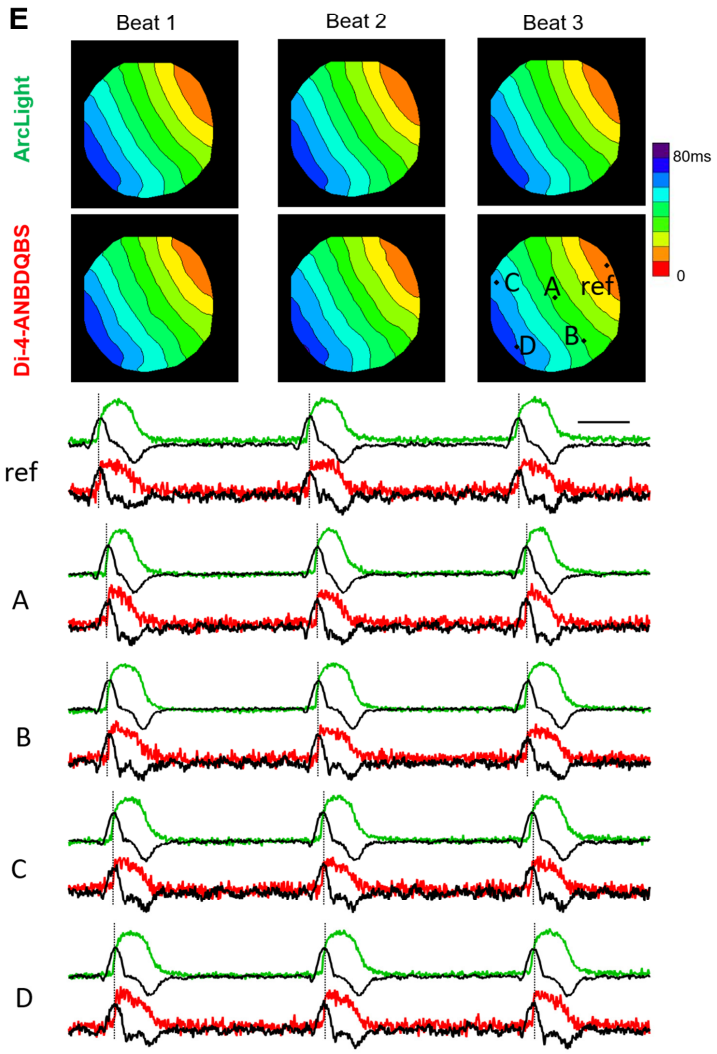

SUPPLEMENTAL FIGURE 2

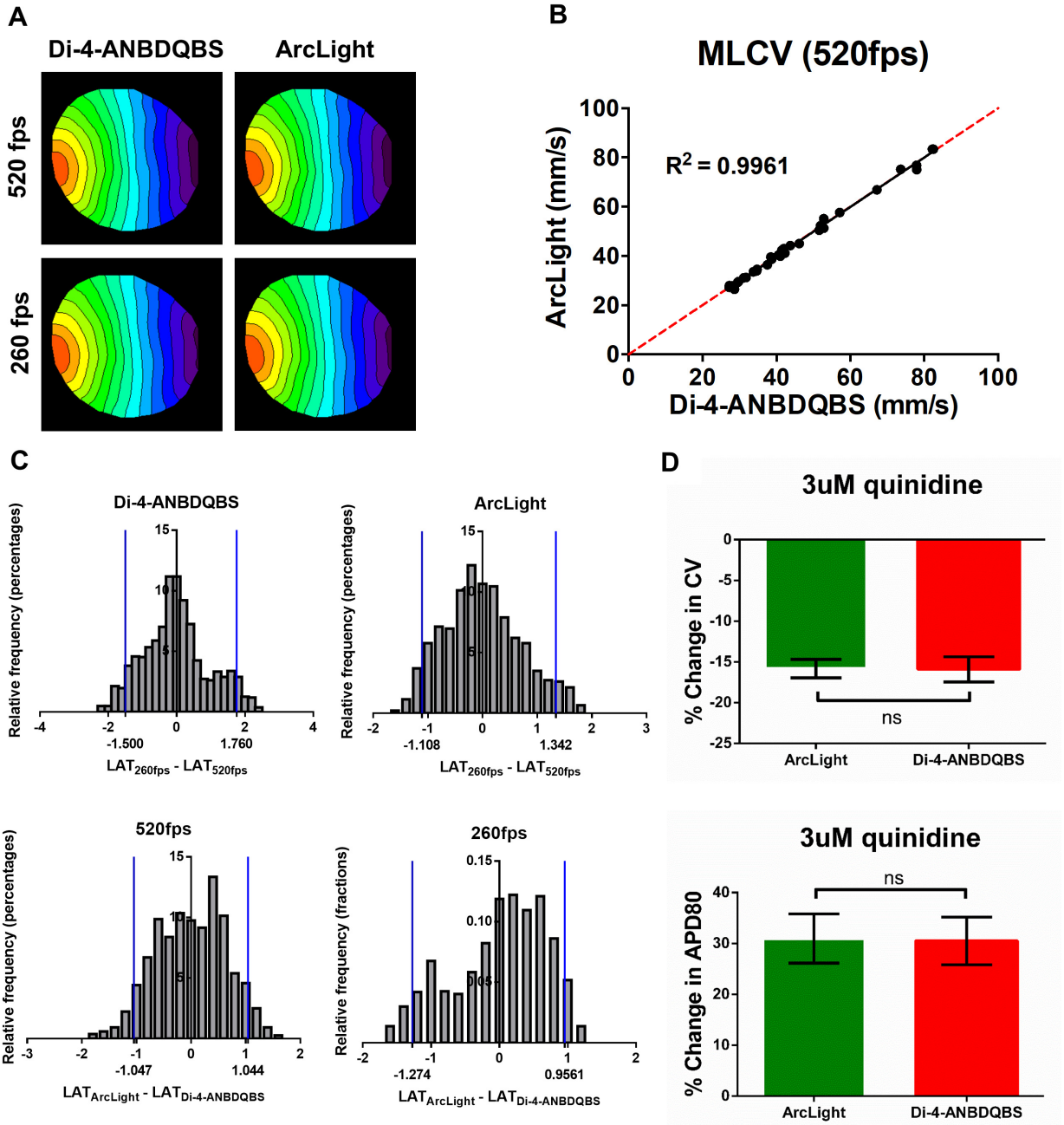

SUPPLEMENTAL FIGURE 3

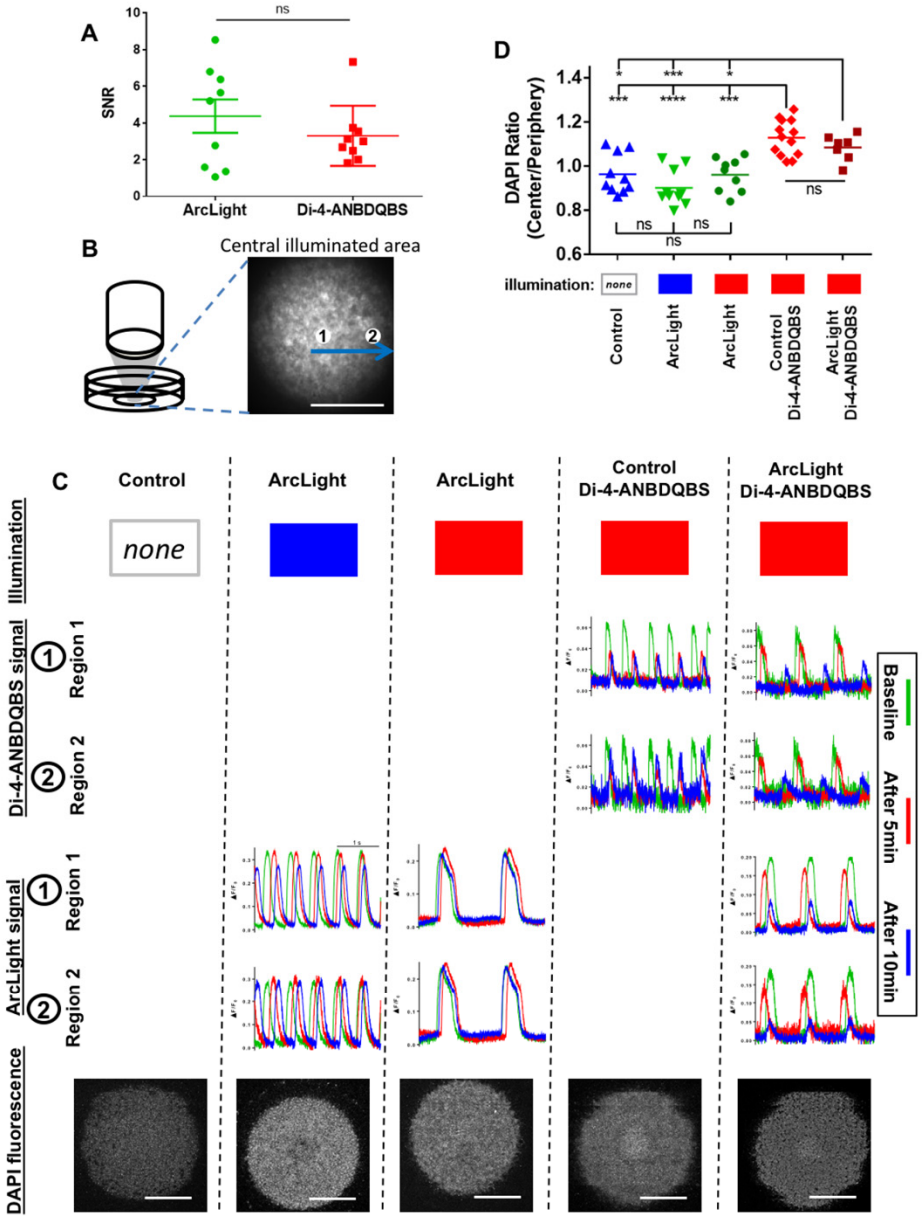

SUPPLEMENTAL FIGURE 4

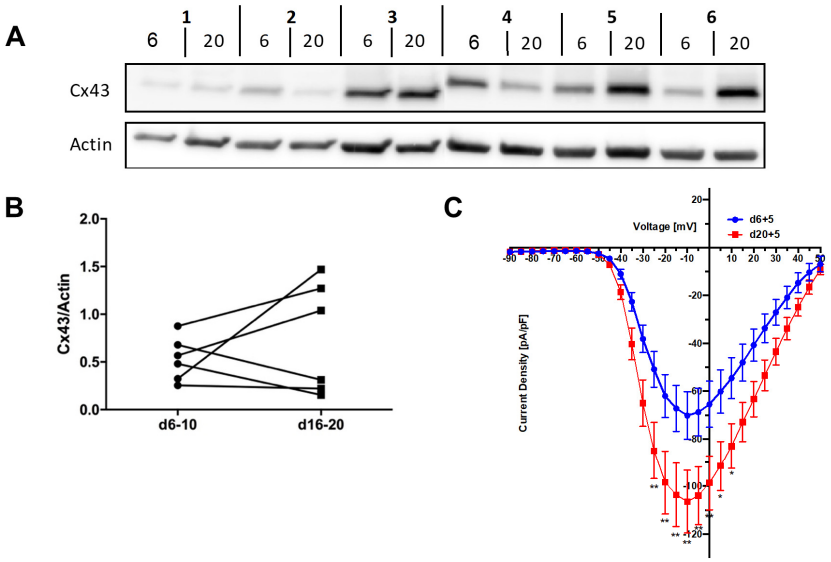

SUPPLEMENTAL FIGURE 5

Legends for Supplemental Figures

Figure S1. ArcLight-hiPSC-CCSs characterization: Flow cytometry, macroscopic view and immunostainings. Related to Figure 1. **[A]** Flow cytometry was performed to evaluate ArcLight-hiPSC differentiation efficiency using cTnT as cardiomyocyte marker (blue); red, unstained. Efficiency of >85% cardiomyocytes (cTnT+) was set as a prerequisite to generate hiPSC-cardiac cell-sheets (hiPSC-CCSs). **[B]** Macroscopic view. Due to the relative high density of seeded cells within the cardiac cell-sheets, the tissue can be visualized macroscopically. The typical approximate diameter of the seeded hiPSC-CCSs was about 5mm. **[C]** Changes in cell content per hiPSC-CCS (n=12 in 3 independent experiments) over time, with time-points of d0 (seeding point), d1, 6-10d, and 16-20d post-plating. **[D]** Top-view of 3D fluorescence stack. **[E]** Side-view of high-magnification of the yellow box from panel A. **[F]** Angle-view of 3D surface reconstruction. **[G]** Orthogonal view of fluorescence confocal planes. Dotted (right) and dashed (top) boxes show z-planes of the dotted and dashed lines, respectively. Red color represents sarcomeric α-actinin, green represents Cx43, and blue represents nuclei (DAPI). White scale-bars represent 50μm.

Figure S2. Experimental design and analysis of ArcLight and Di-4-ANBDQBS comparison. Related to Figure 1 and Experimental Procedures -Electrical stimulation and arrhythmia induction.
[A] ArcLight-hiPSC-CCSs were loaded with dye (Di-4-ANBDQBS), mounted on the heated macroscope stage to reach equilibrium and pacing electrodes were fixed. Pacing was initiated with the desired frequency, and then upon reaching steady state (at least 20 beats), the tissue culture was first imaged with one reporter's filter cube (either ArcLight or Di-4-ANBDQBS), and subsequently, the filter cube was manually swapped (using a revolver array installed on the macroscope) to the second reporter's filter cube. Delay between the two movies acquired (one for each reporter) is estimated to be less than one. **[B-D]** Pacing and incubation modes: **[B]** Bipolar pacing with top-access to tissue (incubator cover open). **[C]** Unipolar pacing with electrodes fixed (incubator cover closed). **[D]** Set-up for bi-phasic electrical cardioversion (incubator cover closed). **[E]** Arclight (green) and Di-4-ANBDQBS (red) optical AP signals. Local activation time (LAT, dashed lines) was defined as the time-point of the maxima of the AP 1st derivative (black) and resulted in similar activation maps (above two rows).

Figure S3. Reliability of ArcLight based optical mapping at high sampling interval (520) and in predicting drug response. Related to Figures 1-3
[A] Activation maps of the same ArcLight-hiPSC-CCS loaded with Di-4-ANBDQBS, generated from analysis of Di-4-ANBDQBS (left) and ArcLight (right) imaging at sampling rates of 520 (top) and 260 (bottom) frames per second (fps). **[B]** Correlation between MLCV values, as measured from ArcLight and Di-4-ANBDQBS recordings in the same cultures imaged at 520fps. Cultures from different developmental stages (6-35d) that were paced at variable rates (CLs: 300-2000ms) were used for analysis. Notice the high correlation (R^2=0.9961, n=33 in 6 independent experiments) between the two reporters. **[C]** Histogram-plots of differences in LAT values at each pixel of the activation maps shown in (A). The top-panel plots compare LAT values (LAT_{260fps}-LAT_{520fps}) derived from each reporter using different sampling rate (260 or 520fps). The bottom-panel plots compare LAT values ($LAT_{ArcLight}$-$LAT_{Di\text{-}4\text{-}ANBDQBS}$) of each sampling rate between the two reporters (ArcLight and Di-4-ANBDQBS). Vertical blue lines represent 5 and 95% percentiles. **[D]** Comparison of the change (in percent) in MLCV and APD_{80} following quinidine administration (n=5 in 3

independent experiments) as measured by Arclight (green) and Di-4-ANBDQBS (red) optical signals.

Figure S4. ArcLight versus Di-4-ANBDQBS: SNR and phototoxicity. Related to Figure 1. **[A]** SNR of ArcLight and Di-4-ANBDQBS signals obtained from the same pixels in the same hiPSC-CCSs ($P>0.05$, paired t-test, n=9). **[B]** Illustration (left) to indicate central illuminated area (shadowed), and high magnification of the illuminated region (right) of one ArcLight-hiPSC-CCS. Two selected ROIs are demonstrated from the central illuminated area (1 and 2). Scale bar = 1mm. **[C]** Optical signals (upper panels) obtained over 10min of continuous central illumination from two illuminated ROIs (1 and 2) and corresponding images of DAPI fluorescence intensity (lower panel) after 20min illumination and incubation with DAPI. Groups (left-to-right): non-illuminated control hiPSC-CCS, blue-illuminated ArcLight-hiPSC-CCS, red-illuminated ArcLight-hiPSC-CCS, red-illuminated Di-4-ANBDQBS loaded control hiPSC-CCS and red-illuminated Di-4-ANBDQBS loaded ArcLight-hiPSC-CCS. Note the decrease in both ArcLight and Di-4-ANBDQBS signals in the two groups loaded with Di-4-ANBDQBS. Green, red and blue colors represent optical signals acquired at baseline, 5min and 10min of illumination, respectively. Scale bar = 3mm. **[D]** Ratio of DAPI fluorescence concentration between illuminated areas and non-illuminated surroundings (one-way ANOVA followed by Tukey post-hoc analysis, $n\geq7$ for each group). **** $P<0.0001$, *** $P<0.001$, ** $P<0.01$, * $P<0.05$.

Figure S5. Evaluation of Cx43 protein content and Na^+ currents. Related to Figure 2. **[A]** Western-blot experiments of Cx43 (n=6). **[B]** Summary of western-blot analysis. **[C]** Comparison of Na^+ activation current density (pA/pF) between cardiomyocytes obtained from hiPSC-CCSs at day 6 (blue) and day 20 (red). ($P<0.05$, n=13,15, Repeated-measurements two-way ANOVA). Error bars represent SEM. *$P<0.05$, **$P<0.01$ when comparing individual current densities at the same voltage (Sidak post-hoc analysis).

Legends for Supplemental Movies

Movie S1. ArcLight versus Di-4-ANBDQBS mapping comparison. Related to Figure 1.
Dynamic optical mapping displays showing action-potential propagation using ArcLight (green) or Di-4-ANBDQBS (red) fluorescence from the same ArcLight-hiPSC-CCS loaded with Di-4-ANBDQS and paced at 1 Hz.

Movie S2. Spiral-wave induction by DC current injection. Related to Figure 4 and Movie S3.
Fluorescence movie of spiral-wave (rotor) induction via DC current injection.

Movie S3. Phase-mapping of spiral-waves (rotors). Related to Figure 4 and Movie S2.
Fluorescence (upper-row) and phase (lower-row) movies of rotors induced in ArcLight-hiPSC-CCSs as acquired using the ArcLight fluorescence channel.

Movie S4. Termination of arrhythmia by electrical cardioversion. Related to Figure 5, Movies S3 and S5.
Fluorescence (left) and phase (right) movies of arrhythmia termination by 50ms field stimulation. Snapshots and analysis described in Figure 5 and in the main text.

Movie S5. Termination of arrhythmia by over-drive pacing. Related to Figure 5 and Movies S3-4.
Fluorescence (left) and phase (right) movies of arrhythmia termination by over-drive pacing. Snapshots and analysis described in Figure 5 and in the main text.

Movie S6. Dofetilide-induced arrhythmogenesis #1. Related to Figures 6-7 and Movies S7-8.
Fluorescence movie of arrhythmia induction by introduction of high dose of dofetilide (50nmol/L). Snapshots and analysis described in Figure 6 and in the main text.

Movie S7. Dofetilide-induced non-propagating EADs. Related to Figures 6-7, Movies S6 and S8-9.
Fluorescence movie showing non-propagating EADs caused by introduction of high dose of dofetilide (50nmol/L).

Movie S8. Dofetilide-induced propagating TA. Related to Figures 6-7, Movies S6-7 and S9.
Fluorescence movie showing propagating TA caused by introduction of high dose of dofetilide (50nmol/L).

Movie S9. Dofetilide-induced arrhythmogensis #2. Related to Figures 6-7 and Movies S6-8.
Fluorescence movie showing TA leading to stable arrhythmia (TdP) induction after the introduction of high dose of dofetilide (50nmol/L).

Supplemental Expanded Experimental Procedures

Maintenance of hiPSCs and cardiomyocyte differentiation

Cardiomyocyte differentiation was induced using the monolayer differentiation system (Burridge et al., 2014; Shinnawi et al., 2015). Colonies of hiPSCs were cultured on 1:200 growth factor–reduced Matrigel (Cultrex) using hESC mTeSR-1 cell culture medium (StemCell Technologies). Cells were passaged via dissociation with 0.5mM EDTA (Invitrogen) in D-PBS without $CaCl_2$ or $MgCl_2$ (Sigma-Aldrich) for 7 minutes at room temperature every 4-6 days, and replated in mTeSR medium supplemented with 2μmol/L of the ROCK inhibitor Thiazovivin (Cayman Chemicals) for the first day following passaging.

To induce differentiation, three to five days after passaging or when the cells reached 80-90% confluence (day 0 of differentiation), the culture-medium was switched to a differentiation medium CDM3 [RPMI-1640 (Gibco), recombinant human serum albumin 500μg/mL (Oryzogen), 213μg/mL, L-ascorbic acid 2-phosphate (Sigma-Aldrich), 1% penicillin/streptomycin (100 U/ml and 100 g/ml, respectively; Biological Industries)], supplemented with 6μmol/L CHIR99021 (Stemgent) for two days. On day two, medium was replaced to CDM3 medium (without CHIR) supplemented with 2μmol/L WNT-C59 (Selleckchem) for additional two days. From day 5 onwards, the cells were cultured with CDM3 medium, and medium was refreshed every other day.

On day 8-10, spontaneous contraction could be identified in the differentiating monolayers. Flow cytometry was performed routinely to ensure >85% cardiomyocyte purity by analyzing the percentage of cells that expressed cTNT (Figure S1A).

Calibration of seeding density

We aimed to obtain functional arrhythmias within our tissue cultures and to minimize the chance of anatomic reentry, thus we decided to seed the cells at maximum viable seeding densities, as it gave rise to minimum number of structural "holes". Variable approximate seeding densities were tried, and we noticed massive cell death at seeding densities higher than 56,000 cells/mm^2 as indicated by floating debris at d1 following cellular-sheet generation. Therefore, we decided to continue with seeding densities of 38,000-56,000 cells/mm^2, and discarded every hiPSC-CCS that contained microscopically-observed areas with no seeded cells ("holes").

Generation of the hiPSC-derived cardiac cellular sheets (hiPSC-CCSs)

Differentiating monolayers of hiPSC-CMs of >85% $cTnT^+$ purity at d8-14 post-differentiation were enzymatically dissociated using TrypLE 1x (ThermoFisher Sientific), passed through a 100μm strainer to obtain single-cell suspensions, and seeded as large-scale (~0.5cm diameter) circular cell-sheets on recently-dried Matrigel-coated culture-plates (Corning) at a seeding

density of 38,000-56,000 cells/mm^2 (0.75-1.1 million cells in 50µl drop, Figure S1B), in RPMI/B27 (B27 supplement minus insulin, Gibco) culture medium containing 1% penicillin/streptomycin and blebbistatin [(Lee et al., 2012), 5µmol/L, Sigma-Aldrich].

We found that the factors crucial to achieve robust and efficient CCSs generation included:

(1) The use of only efficient hiPSC cardiomyocyte differentiations (resulting in >85% cTnT$^+$ differentiating cells), which is probably the most important factor; (2) The use for cell dissociations of relatively early hiPSC-CMs (before 14d of differentiation); (3) The use of single-cell suspensions following enzymatic dissociations, as we noticed that this improves the homogeneity of the generated CCSs; and (4) The use of a cell strainer (maximum 100µm). These issues were determined after a long optimization and calibration period. Only after mastering the technique and achieving robust and homogenous results in each session, did we move to perform all the experiments described in this study.

Strict adherence to this protocol yielded 80-90% successful independent-sessions, and in each successful independent-session more than 90% of the generated hiPSC-CCSs were without any structural discontinuities.

Time-dependent cell content analysis:

The generated hiPSC-CCSs were enzymatically dissociated using TrypLE 1x (ThermoFisher Sientific) and their cell content was counted using a simple hemocytometer at different time-points: d0 (seeding point), d1, d6-10, and d16-20 post-plating.

Flow cytometry

For differentiation efficiency evaluation, post-differentiation ArcLight-hiPSC-derived monolayers were routinely dissociated using TrypLE at 37°C, fixated using 4% paraformaldehyde in PBS, permeabilized with Saponin buffer (0.5% Saponin, 5% FBS in PBS) for 10min at RT, stained with primary antibody mouse anti-cardiac troponin T for 30min in 4°C (1:1000, Invitrogen, MA512960), then with secondary antibody donkey anti-mouse IgG-Cy3 for 30min at room temperature, and filtered using 40µm cell strainer before flow cytometry analysis. Analytical flow cytometry was performed using LSR Fortessa II flow cytometer (BD Biosciences), and analysis was carried out through FlowJo software.

Immunostaining studies

hiPSC-CCSs cultured on 20mm matrigel-coated glass-bottom dishes (MatTek), fixed with 4% paraformaldehyde (Bio-Lab) for 20 minutes at room temperature, washed three times in PBS, permeabilized with 1% Triton (Sigma-Aldrich) for 10min at room temperature, blocked with

5% horse serum (Gibco) for 1 hour in room temperature, and incubated overnight at 4°C with the primary antibody for sarcomeric α-actinin (1:100; mouse; Sigma-Aldrich, A7811), and for connexin-43 (1:100; Rabbit; Santa Cruz Biotechnology, sc-9059). The specimens were washed three times (each for 5 minutes) with PBS and incubated for 1 hour at room temperature in the dark with the following 1:150 diluted secondary antibody: Cy3 donkey anti-mouse IgG (715-175-150, Jackson Immunoresearch laboratories), and Cy2 donkey anti-rabbit IgG (711-225-152, Jackson Immunoresearch laboratories).
Primary and secondary antibodies were diluted in PBS containing 3% horse-serum and 0.1% Triton. Nuclei were counterstained with DAPI (1:500, Sigma-Aldrich, D9564). The preparations were examined using a Zeiss LSM-710 laser-scanning confocal microscope (Zeiss). 3D reconstruction of fluorescence z-stacks, intensity-threshold surface reconstruction, and orthogonal confocal planes were generated using Imaris software (Bitplane).

Voltage sensitive dye (VSD) loading

For experiments including comparison between ArcLight and Di-4-ANBDQBS, ArcLight-hiPSC-CCSs were loaded with fresh RPMI/B27 medium containing 15µg/ml (26.3µmol/L) Di-4-ANBDQBS (Purchased from Prof. Leslie M. Loew, U.S), at room temperature in the dark for 7min, washed twice with PBS, then the medium was switched to Tyrode's solution for further assessment. Following experimental procedures, Di-4-ANBDQBS loaded cellular-sheets were discarded, and were not used for further experimentation.

Optical mapping

The optical mapping setup consisted of a high speed EMCCD camera (Evolve® 512 Delta, Photometrics, 512x512 pixels) mounted on a fluorescent macroscope (MVX10, Olympus) equipped with 0.25 NA 6.3X - 63X (MVPLAPO 1X, Olympus, used for almost all experiments) and 0.5 NA 12.5X - 125X (MVPLAPO 2XC, Olympus, used only for DAPI viability assay, see below Evaluation of phototoxicity) objectives. The default field of view (FOV) achieved for illumination and imaging by using the 1X objective and setting the zoom body on 2.5X was 10mm. However, for focused central excitation in the phototoxicity experiments, the 2X objective and 6.3X in the zoom body were used to achieve ~2mm FOV. Both ArcLight and Di-4-ANBDQBS containing specimens were excited using LEDs (X-Cite® TURBO, Excelitas Technologies) with peak wavelengths at 475 and 630 nm, respectively. For ArcLight recordings, emission was passed through 495 long-pass dichroic mirror and filtered using 525/50 band-pass filter. While a 660 long-pass dichroic mirror and 665 long-pass filter were used for Di-4-ANBDQBS recordings (All from Chroma). Fluorescence was acquired at 4x4 binning, and a sampling interval of 3.847ms (~260 frames per second) at all experiments. To compare mapping results at different sampling rates we acquired the data for

both ArcLight and Di-4-ANBDQBS also at a sampling interval of ~1.923ms (520 frames per second, 8x8 binning).

ArcLight vs. Di-4-ANBDQBS mapping comparison

ArcLight-hiPSC-CCSs were loaded with Di-4-ANBDQBS and both reporters were imaged by alternating filter cubes using the optical mapping setup as described above. To compare the accuracy of the electrophysiological parameters (APD_{80} and MLCV values) derived using the two reporters, we evaluated cultures at different developmental stages (6-35d) and at various pacing frequencies (CLs: 300-2000ms) (Figure S2A). Pacing was initiated with the desired frequency, and then upon reaching steady state (at least 20 beats), the tissue culture was first imaged with one reporter's filter cube (either ArcLight or Di-4-ANBDQBS), and subsequently, the filter cube was manually swapped (using a revolver array installed on the macroscope) to the second reporter's filter cube. Delay between the two movies acquired (one for each reporter) was estimated to be less than one second.

Evaluation of signal-to-noise ratio (SNR)

To compare SNR for ArcLight and Di-4-ANBDQBS imaging, we first performed a series of preliminary studies to determine the optimal loading conditions (concentration and incubation time) of Di-4-ANBDQBS. This calibration results in optimal loading conditions of 60µg/mL for 20min at room temperature. Next, from each 8 seconds recording of ArcLight-hiPSC-CCSs loaded with Di-4-ANBDQBS and paced at 1Hz, we sampled one random pixel for analysis. Fluorescence signal was inverted and normalized (transformed to $\Delta F/F_{min}$) for further analyses. For each AP, $(\Delta F/F)_{baseline}$ was calculated as the average of 50ms diastolic segment (100ms to 50ms prior to AP activation time) and the amplitude was defined as $(\Delta F/F)_{peak}$-$(\Delta F/F)_{baseline}$. SNR was defined as the amplitude divided by the root-mean-square of the baseline segment (SNR_A, Figure S4A). Likewise, SNR was calculated using four additional formulas based on the derived ΔF/F signal ($SNR_{B\text{-}E}$, data not shown)

$$SNR_A = \frac{Amp}{RMS_{baseline}};\ SNR_B = \frac{Amp}{SD_{baseline}};\ SNR_C = \frac{Amp}{\sqrt{\frac{VAR_{baseline}}{n}}};$$

$$SNR_D = \frac{RMS_{peak} - RMS_{baseline}}{RMS_{baseline}};\ SNR_E = \frac{RMS_{peak}}{RMS_{baseline}}$$

RMS = root mean square; SD = standard deviation; VAR = variance. Baseline = 50ms diastolic segment (100ms to 50ms prior to activation time); Amp: peak value minus baseline mean; n = number of frames of the baseline segment (in our case: 26).

Evaluation of phototoxicity

The central portion (2mm diameter) of the hiPSC-CCSs was continuously illuminated with

blue- (475nm, 12mW, “ArcLight alone” hiPSC-CCSs) **or** red- (670nm, 12mW, "ArcLight alone", "ArcLight + Di-4-ANBDQBS" and "Di-4-ANBDQBS alone") excitation lights for 20 min. hiPSC-CCSs not expressing either reporters nor illuminated were used as a control group [used from the original hiPSC-cell line prior to the transgenic introduction of Arclight (Shinnawi et al., 2015)]. In some of the cultures, we also performed optical recordings at baseline and at 5 and 10 minutes following the initiation of illumination. At the end of the illumination period, the specimens from all five groups were incubated with 1:500 DAPI (Sigma-Aldrich) in PBS at room temperature for 3 minutes, washed with PBS and imaged with Zeiss LSM-710 laser-scanning confocal microscope. DAPI concentration (fluorescence intensity normalized per area) ratio between central (illuminated) and peripheral (non-illuminated) regions was calculated for each hiPSC-CCS ("DAPI center/periphery ratio"). DAPI emission was collected by whole hiPSC-CCS scanning using 5x5 array of 1024x1024 pixel frames to give 6x6mm full frames. In addition, DAPI concentration (fluorescence intensity normalized per area) ratio between central (illuminated) and peripheral (non-illuminated) regions was calculated for each hiPSC-CCS (DAPI center/periphery ratio).

Acquisition and analysis of electrophysiological parameters

Platform for signal processing and data analysis: Micro-Manager was used for acquisition in the SNR, phototoxicity and acquisition speed comparison experiments. For all other experiments, OMProCCD (Huang et al., 2016; Kim et al., 2015), a custom-designed software based on Interactive Data Language (IDL 8.5; Exelis Visual Information Solutions, received as a generous gift from Prof. Bum-Rak Choi, Brown University) was utilized for acquisition and analysis.

Excluding bad pixels: bad pixels were discarded by both threshold-based automatic and manual exclusion; only relevant pixels, which resembled tissue-filled area, were analyzed.

Filtration: data was filtered using spatial smooth filter (3x3 pixels), then, using polynomial temporal filter (3^{rd} order, 13 points window size). Similarly, polynomial temporal filter was also applied on the first derivative dF/dt (3^{rd} order, 30 points window size).

Calculation of local activation time (LAT), APD_{80}, conduction velocity (CV) and their related maps: LAT for each electrical wave at a specific pixel was determined as the time-point of maximal 1^{st} derivative $(dF/dt)_{max}$. Local APD_{80} was used as a surrogate for APD (Herron, 2016; Hou et al., 2010; Muñoz et al., 2007) and was determined as the time interval between LAT and time-point of 80% repolarization of the optical action potential. Local CV vector was calculated as the distance of action potential propagation over time-intervals calculated from LATs of 5x5 square of pixels and assigned to the central relevant pixel. Activation, APD_{80} and CV maps were subsequently generated by plotting colored local activation time values, local APD_{80} values and local CV values of all relevant pixels per beat. Averaged maps

for the same parameters were generated for each recording by averaging at least 4 beats. Mean local CV (MLCV), and mean APD_{80} were calculated as the mean of all relevant pixel values per recording.

Pharmacological studies and solutions

For single-dose experiments (carbenoxolone), recordings were performed in Tyrode's solution at 30 minutes post drug administration. For all other drug studies, long (1>hour) dose-response experiments were performed while maintaining hiPSC-CCSs in fresh culture medium (RPMI/B27) and incubated in 95% air, 5% CO_2 (200ml/minute). Recordings were acquired 10 minutes after the administration of each dose. Tyrode's solution contained (in mmol/L): NaCl-140, KCl-5.4, $CaCl_2$-1.8, $MgCl_2$-1.0, HEPES-10 and glucose-10 (pH-7.4 with NaOH). Carbenoxolone (working concentration: 50µmol/L), quinidine (0.1, 0.3, 1, 3, 10 and 30µmol/L) and lidocaine (1, 3, 10, 30, 100 and 300µmol/L) stock solutions were dissolved in H_2O, while dofetilide (0.3, 0.3, 1, 3, 10, 30 and 100nM) stock solution was dissolved in DMSO. All drugs were purchased from Sigma-Aldrich.

Electrical stimulation and arrhythmia induction

A stimulus isolation unit (SIU-102, Warner-instruments) was utilized to deliver 5ms pulses through a platinum iridium electrode (Alpha-Omega, Figure S2B) or custom-made platinum electrodes positioned close to the tissue edge (Figure S2C) at varying pacing frequencies (300-2000ms cycle-lengths [CLs] for MLCV and APD comparison between ArcLight and Di-4-ANBDQBS. 1000, 800, 600 and 500ms CLs to derive restitution curves). Arrhythmia inducibility was evaluated using a three-step-pacing protocol: (1) Incremental pacing frequency (CLs-1000, 800, 600, 500, 400, 300, 250, 200ms) until loss of capture or induction of arrhythmia (maximum stimulation current intensity was set to 3x of 1 Hz 100% capture threshold); (2) Burst pacing (20ms intervals, 5ms stimulus duration, 3x threshold) for 3s; and if arrhythmia was not initiated (3) DC current injection for up to 3s (3x threshold).

Phase mapping

Phase-maps and related rotor biophysical parameters were computed similarly to that described previously (Gray et al., 1998; Iyer and Gray, 2001; Pandit and Jalife, 2013) using a semi-automated custom-written MatLab script. The code contains an algorithm, which loads a fluorescence-images stack of at least two rotor rotations as an input, and plots the fluorescence of each pixel versus the fluorescence of the same pixel in a consecutive frame within an approximate interval of $0.25APD_{80}$.

The phase at a certain time-point for each pixel is derived as the rotation angle (in radians, between $-\pi$ and π) observed in the plot of the two fluorescence values around the

mean. This allows the generation of two-dimensional color-coded phase maps representing the phase values at each pixel. Singularity points (SPs) were identified as the points where all phases conjoin (Iyer and Gray, 2001). Meandering pathway of the SP was calculated as the sum of distances that the SP moves in 6 steps of one rotor rotation. Wave-front and wave-tail were defined as two continuous lines, which connect pixels having phase values between -1.85 and -1.75 rad (for wave-front), and between 3.1 and 3.14 rad (for wave-tail). Rotor radius, which is inversely-proportional to curvature, was obtained as previously described (Hou et al., 2010; Muñoz et al., 2007). From a representative snapshot of the phase stack, the tangent of the SP was computed by linear regression of the wave-front pixel locations in the immediate vicinity of the SP (closest 6-15 identified pixels of wave-front including the singularity point), and a perpendicular line was extended from the SP to cross the wave-front. The length of the perpendicular line was defined as rotor radius.

Dofetilide-induced arrhythmia, rapid pacing and $MgSO_4$ arrhythmia prevention experiments

High dose dofetilide (50nmol/L) was administered either alone or in combination with 2.1mmol/L $MgSO_4$. hiPSC-CCS were continuously paced at 0.2Hz throughout the experiment. For rapid pacing experiments, hiPSC-CCSs treated with dofetilide (50nmol/L) and pacing at 1-1.25Hz (1000-800s CL). The electrical activity in the cultures was closely monitored and the resulting arrhythmogenicity was classified and scored as either the development of non-propagating EADs (Movie S7, arrhythmogenic score-1), isolated propagated TA (Movie S8, score-2), or the development of stable re-entrant activity (Movies S6 and S9, TdP, score-3).

Western-blot

hiPSC-CCS on days 6 and 20 post plating were lysed with ice-cold RIPA lysis buffer and protease inhibitor (Sigma). 40µg of protein from the samples were mixed and resolved in 4x Laemmli Sample Buffer (BioRad) and incubated in 37°C for 40 minutes before loading on polyacrylamide gels (Bio-Rad). The electrophoresed proteins were transferred to PVDF membranes (Bio-Rad). The membranes were incubated for 60 minutes with 3.5% dry milk (Santa Cruz) and Tris-buffered saline (TBST) to block nonspecific binding sites. The specific primary antibodies used for detection of antigens of interest: anti Nav1.5 (1:400 in 5% BSA in TBST, alomone ASC-013), anti α-actinin (1:2500 in 3.5% milk in TBST, sigma A7811), anti Cx43 (1:500 in 5% BSA in TBST, Santa Cruz sc-9059), anti β-actin (1:1000 in 3.5% milk in TBST, Abcam 8224). The membrane was incubated with the primary antibodies over-night at 4°C and secondary antibodies for 2h at room-temperature (BioRad, 1:5000 in 3.5% milk in TBST). Primary antibody incubation followed by HRP-coupled secondary antibodies

(BioRad). Proteins were revealed with ECL Prime (BioRad) and images were acquired using a LAS4000 Camera (GE Healthcare). For quantitation, band intensities were measured using ImageJ.

Sodium currents measurements

Paired (generated at the same dependent-session) hiPSC-CCSs on days 6 and 20 post plating were enzymatically dissociated and re-plated as single cells on Matrigel-coated glass bottom dishes (MatTek). Sodium currents (I_{Na}) were recorded 5 days post plating from single hiPSC-CMs using the whole-cell patch clamp technique at voltage-clamp mode. Data was amplified, acquired and analyzed using MultiClamp 700B, Digidata 1440A and pClamp10, respectively. Whole-cell capacitance along with series resistance compensation (≥75%) was applied and I_{Na} currents were elicited by applying 50ms depolarizing steps from a holding potential of -90mV to voltages between -90 and 50mV in 5mV increments. Experiments were performed at room temperature with extra-cellular solution consisting of (in mmol/L): NaCl-140, CsCl-5.4, $CaCl_2$-1.8, $MgCl_2$-1, glucose-10, HEPES-10, and nifedipine-0.01 (pH-7.4 with CsOH) while the pipette solution consisted of (in mmol/L): NaCl-3, CsCl-133, $MgCl_2$-2, Na_2ATP-2, TEA-CL-2, EGTA-10, HEPES-10, (pH-7.3 with CsOH). Data was digitized at 20 KHz and filtered using 5 KHz low-pass filter.

Statistical analysis

Data is presented as mean±SEM. Paired t-test was used to compare ArcLight- and Di-4-ANBDQBS- derived MLCV, APD_{80} and SNR values as well as changes in mean MLCV and APD_{80} values following carbenoxolone (50µmol/L) and quinidine (3µmol/L) administration. Repeated-measurements one-way ANOVA followed by Tukey post-hoc multiple-comparison analysis was carried out for comparison of mean MLCV and APD_{80} values in: (1) repeated-phenotyping experiments over time, (2) in pharmacological dose-response experiments and (3) in the dofetilide±$MgSO_4$ APD studies. Similalry, Repeated-measurements one-way ANOVA followed by Tukey post-hoc multiple-comparison analysis was carried out for DAPI ratio comparisons. Repeated-measurements two-way ANOVA followed by Sidak post-hoc analysis was carried out for Na^+ activation currents analysis. Kruskal-Wallis test followed by Dunn's multiple comparison test was carried out for arrhythmogenicity score comparisons.

Supplemental References

Burridge, P.W., Matsa, E., Shukla, P., Lin, Z.C., Churko, J.M., Ebert, A.D., Lan, F., Diecke, S., Huber, B., Mordwinkin, N.M.*, et al.* (2014). Chemically defined generation of human cardiomyocytes. Nat Methods *11*, 855-860.

Gray, R.A., Pertsov, A.M., and Jalife, J. (1998). Spatial and temporal organization during cardiac fibrillation. Nature *392*, 75-78.

Herron, T.J. (2016). Calcium and voltage mapping in hiPSC-CM monolayers. Cell Calcium *59*, 84-90.

Hou, L., Deo, M., Furspan, P., Pandit, S.V., Mironov, S., Auerbach, D.S., Gong, Q., Zhou, Z., Berenfeld, O., and Jalife, J. (2010). A major role for HERG in determining frequency of reentry in neonatal rat ventricular myocyte monolayer. Circ Res *107*, 1503-1511.

Huang, X., Kim, T.Y., Koren, G., Choi, B.-R., and Qu, Z. (2016). Spontaneous initiation of premature ventricular complexes and arrhythmias in type 2 long QT syndrome. Am J Physiol Heart Circ Physiol *311*, H1470-H1484.

Iyer, A.N., and Gray, R.A. (2001). Experimentalist's approach to accurate localization of phase singularities during reentry. Ann Biomed Eng *29*, 47-59.

Kim, T.Y., Kunitomo, Y., Pfeiffer, Z., Patel, D., Hwang, J., Harrison, K., Patel, B., Jeng, P., Ziv, O., Lu, Y.*, et al.* (2015). Complex excitation dynamics underlie polymorphic ventricular tachycardia in a transgenic rabbit model of long QT syndrome type 1. Heart Rhythm *12*, 220-228.

Lee, P., Klos, M., Bollensdorff, C., Hou, L., Ewart, P., Kamp, T.J., Zhang, J., Bizy, A., Guerrero-Serna, G., Kohl, P.*, et al.* (2012). Simultaneous voltage and calcium mapping of genetically purified human induced pluripotent stem cell-derived cardiac myocyte monolayers. Circ Res *110*, 1556-1563.

Muñoz, V., Grzeda, K.R., Desplantez, T., Pandit, S.V., Mironov, S., Taffet, S.M., Rohr, S., Kléber, A.G., and Jalife, J. (2007). Adenoviral expression of IKs contributes to wavebreak and fibrillatory conduction in neonatal rat ventricular cardiomyocyte monolayers. Circ Res *101*, 475-483.

Pandit, S.V., and Jalife, J. (2013). Rotors and the dynamics of cardiac fibrillation. Circ Res *112*, 849-862.

Shinnawi, R., Huber, I., Maizels, L., Shaheen, N., Gepstein, A., Arbel, G., Tijsen, A.J., and Gepstein, L. (2015). Monitoring human induced pluripotent stem cell-derived cardiomyocytes with genetically encoded calcium and voltage fluorescent reporters. Stem Cell Rep *5*, 582-596.